TITLE: **MOLLER Experiment Downstream Coil Design Type Considerations**

BY: J. Mammei, C. Gal, S. Rahman and R. Fair DATE: 12/13/2020

Intended Checker and Approvers:

CHK: K. Kumar

1. APP: J. Fast

2. APP: C. Keppel

3. APP: R. Ent

REV.	ECO#	DESCRIPTION	BY	CHK.	APP.	APP.	DATE

SUMMARY OF CHANGES FROM PREVIOUS REVISION:

Contents

Executive Summary

The possibility of a “segmented” magnet, with multiple separate coils instead of the “hybrid” magnet with multiple current returns for the downstream toroidal magnet has been suggested by the informal Magnet Review Committees since the first one. Initial attempts to achieve an acceptable focus with such a configuration failed. As long as the same $\int \vec{B} \cdot d\vec{\ell}$ in each segment is the same, and centered at the same z location, then an acceptable detector plane distribution is possible. The issue was that the constraint on the current density at the time was about 1200 A/cm^2. We now understand that the real constraint is not the current density per se, but other parameters such as temperature rise, water flow velocities and pressure drop. We believe we have a segmented design that not only meets the physics requirements, but is also better from an engineering perspective. Therefore we recommend that the segmented configuration for the downstream toroid be accepted as the new baseline.

1. Introduction

This document summarizes the relevant physics and engineering considerations for the choice of a segmented vs hybrid coil configuration, which were entered into a Pugh matrix.

This document is written to accompany the Pugh matrix, which is organized into four main sections related primarily to Design, Fabrication, Assembly and Operation. Below we present information used to choose the weights and scoring in this Pugh matrix for each of these sections. The full Excel-based Pugh matrix excel spreadsheet can be found in the MOLLER document database with relevant extracts provided within the Engineering Criteria section.

2. Physics Criteria

In order for a spectrometer to be acceptable, it has to be able to produce the distribution of the møller electrons that scatter from the electrons in the target (abbreviated as "ee" or referred to as "mollers" throughout this document) as well as the electrons that are elastically and inelastically scattered from the protons in the target (ep and ine, respectively) (see figure 1). Of particular interest is the distribution of the inelastic electrons (not visible in the plot) at the detector plane, due to the relative size of the asymmetry, A_{ine}, despite the relatively small rates. These distributions are produced using a GEANT4 simulation (see section 2.1).

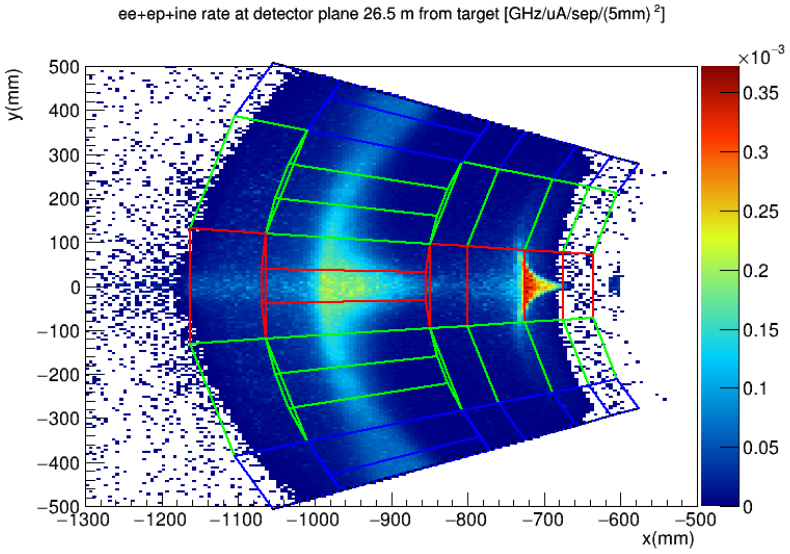

Figure 1 *– 2D rate-weighted distribution of the default configuration for the spectrometer, in a single septant, at the detector plane. The beam centerline is off to the right of the plot at (0,0). The dark blue is very low rate and the dark red is high rate. The pixel size is 5mm^2. The red, green and blue lines give a conceptual picture of the detector array. There are 6 rings with 3 sectors (red is in the open sector, blue is in the closed sector, and green is the transition sector. The moller ring (ring 5) is segmented 3x as much in the azimuthal direction as the other rings. The ep ring is ring 2.*

The spectrometer performance can be understood using theta-r plots (see figure 2). Ideally, a spectrometer would focus all accepted scattering angles in a narrow range of radii. The MOLLER

spectrometer is an open spectrometer (as opposed to a high resolution spectrometer such as those in Hall A and C). In addition, there are a number of constraints on the spectrometer, such as the length of the hall, filling no more than half the azimuth, and being able to successfully water-cool these very long and skinny resistive magnets. Figure 2 shows the rate-weighted theta-r distribution for the default downstream torus. The peak between ~680mm < r < 740 mm is the ep elastic peak. The peak between ~850mm < r < 1020 mm is the moller peak. As you can see, the peaks have quite a curve to them, rather than being narrow vertical stripes.

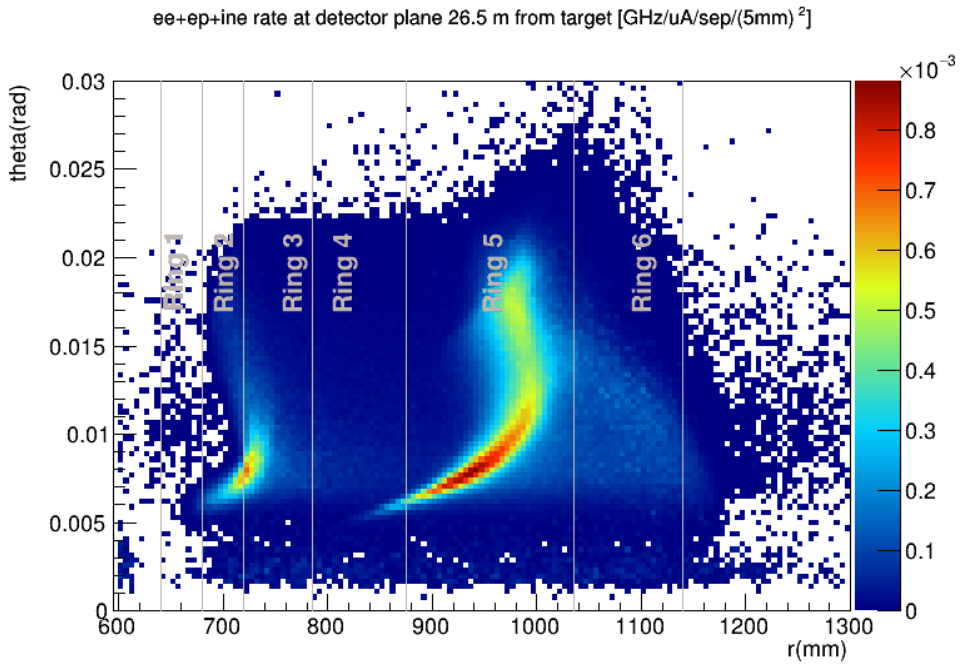

Figure 2 – *Rate weighted theta-r distribution of the default configuration for the spectrometer. An ideal spectrometer would have vertical stripes. This spectrometer is not ideal – it is an "open", and constrained by the available space in the hall. It does a remarkable job of focussing a large range of scattered energies (2-8 GeV for ee and 11 GeV for ep) and angles (approximately 6-20 mrads).*

Figure 3 shows the 1D radial rate and f_iA_i distributions for the moller, ep, and inelastic processes where f_i is the fractional rate, or dilution, and A_i is the asymmetry for each process, i, in each bin. The importance of the inelastics can be seen in the f_iA_i distribution. Due to the large inelastic asymmetry, the relative contribution to the measured asymmetry in a given detector tile can be quite large. This is the driving motivation for the large number of tiles in the detector array. It allows us to have a separation of W regions for the inelastics, which will help us to determine the contribution of the inelastics to the measured asymmetry in the moller ring. We would want any spectrometer to give approximately the same 1D and 2D distributions.

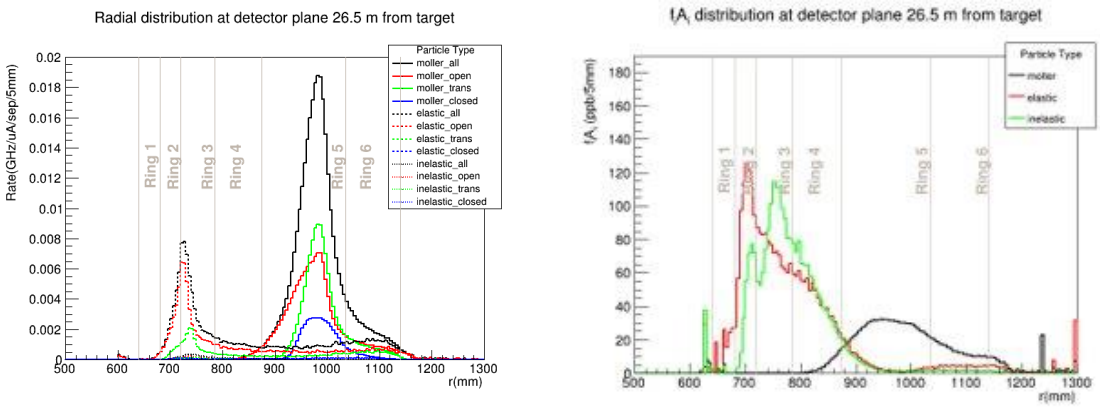

Figure 3 – *1D radial distribution of the rate (GHz/uA/sep/5mm) on the left. The dashed lines are the elastic ep events in the open, closed and transition sectors (red, blue and green respectively) with the sum shown in black. The solid lines are the mollers (same color definitions). The inelastic rate distribution is also being plotted but is not visible on this scale. On the right is the 1D radial distribution of the fractional rate f_i for a given process in each bin, times the mean asymmetry A_i for that process in that bin. The 3 processes here are the moller (black), ep (red) and inelastic (green). Note the relative contribution of the inelastics, due to their large asymmetry. In both plots the approximate radial ring definitions are shown as vertical grey lines.*

There were 4 versions of the downstream torus that were studied for this document; they will be described in section 2.2. They include 3 segmented versions and a hybrid version. The default of a segmented version was chosen a while ago because it gave slightly better physics results. You can see comparisons of all these distributions in the appendix (figures A1 and A2). While the distributions have slightly different features, they all can be made to work with the appropriate choice of detector tiling. The ultimate criteria is the uncertainty on the determination of the moller asymmetry, δA_{ee}, which can only be determined with a full "deconvolution" study, which uses the simulation data in each of the detector tiles to separate out the moller asymmetry and estimate the uncertainty that can be determined during the experiment (see section 2.3). The results of the full deconvolution study confirm that any of the configurations should be adequate for the physics, with appropriate detector tiling.

2.1 Description of the simulations

The collaboration has written and continues to develop a GEANT4 simulation of the experiment, remoll. The simulation includes the geometry which is defined using GDML files which are read in at the beginning of a run. The geometry includes the floor, walls and roof of the hall as well as a model for the beam dump. It includes the target scattering chamber, drift pipe, detector plane and shielding in addition to the conductors of the upstream and downstream toroidal magnets (see figure 4). The fields of the magnets for the various conductor configurations are produced in TOSCA and read in to the GEANT4 simulation. Specific generators are used to simulate 5 million ee events, 10 million ep events and 10 million ine events as well as other background processes for each configuration. The generated primary and secondary events are recorded as hits on a virtual plane at the location of the main detector system. In subsequent analysis, the ring boundaries on the plane are moved around until relative uncertainties extracted via deconvolution are approximately minimized for each configuration.

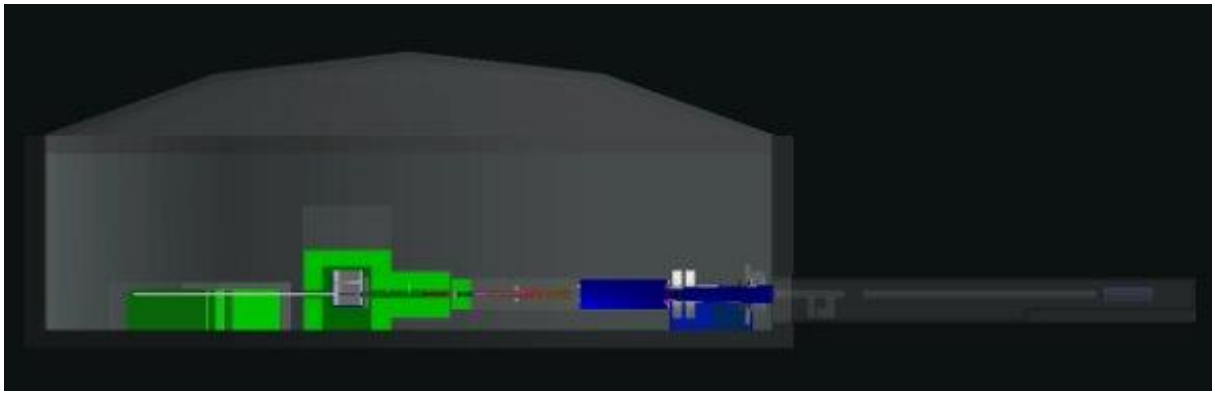

Figure 4 –*The GEANT4 geometry in remoll. The same geometry was used in simulating both cases.*

The JLAB magnet group produces "blocky model" versions of their conductor configurations in TOSCA. The same models are also rendered in CAD (see figure 5). The Manitoba group imports the TOSCA conductor files and produces field maps using a Biot-Savart calculation in TOSCA. The field maps are then imported into the GEANT4 simulation. For the studies presented in this document, the same upstream field map was used for all the simulations. Only the downstream torus had different configurations.

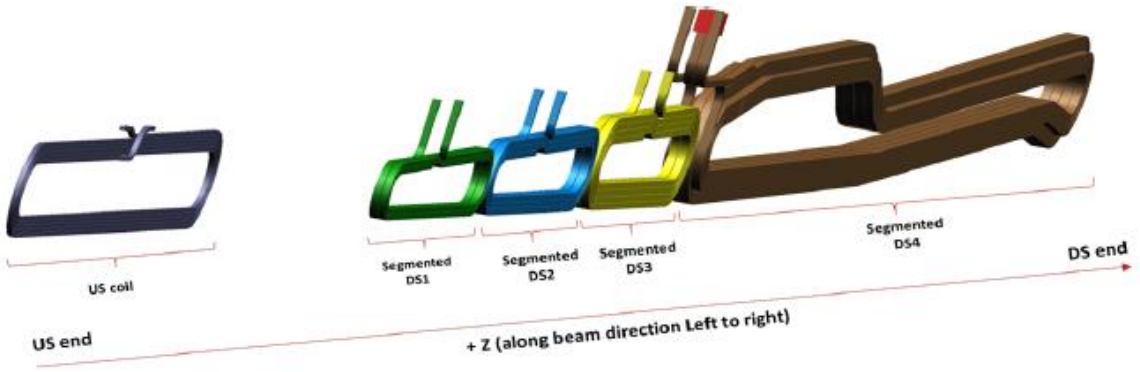

Figure 5 – *CAD drawing of the upstream (grey coil on the left) and downstream toroids in a single septant, in the default configuration. The downstream torus is segmented into 4 separate coils (green, blue, yellow and brown).*

2.2 Comparison of the segmented and hybrid configurations

The "hybrid" version of the spectrometer was developed to fit the necessary $\int \vec{B} \cdot d\vec{\ell}$ in Hall A with a constraint (among others) of less than 1200 A/cm^2 current density. In order to maximize the length of each segment the conductor was laid out so that there was a single coil with multiple current returns. The segmented version of the downstream torus has to have the different current segments centered on the same z location, and have the same total $\int \vec{B} \cdot d\vec{\ell}$, but in a shorter coil. So the total current, or

$\vec{B} \propto NI$, has to be increased to make up for the decrease in the $d\vec{\ell}$. On average, the coils are about 15% shorter. The NI can be increased by using the same conductors and increasing the current (and thus current density) or by optimizing the conductor size (outer dimensions as well as water-cooling hole) and layout.

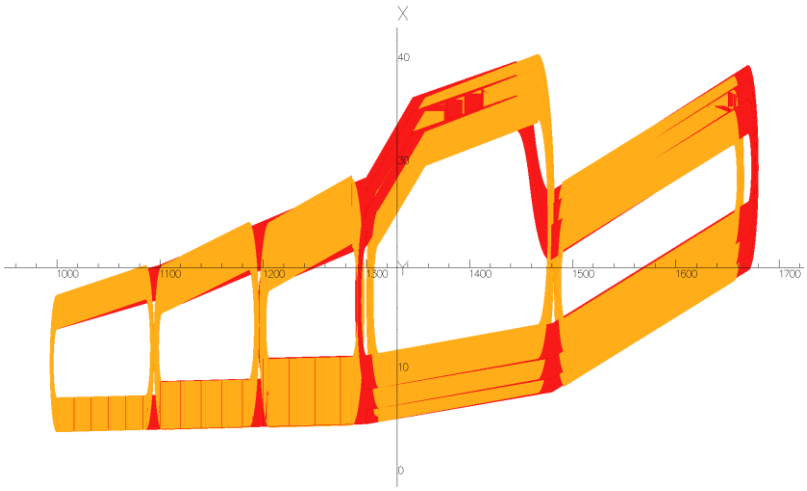

Figure 6 – *Overlay of the Manitoba hybrid (red) and segmented (gold) versions of the downstream torus blocky models in TOSCA to demonstrate the differences. Note the z scale is compressed by a factor of 10. As long as the central z location of each subcoil is the same, and the total NI over the length is the same, the conductor configurations should yield similar physics optics. In order for the* $\int \vec{B} \cdot d\vec{\ell}$ *to be the same, the loss in length has to be made up for by a corresponding increase in current. The segmented coils are on average approximately 15% shorter than those of the hybrid.*

The JLAB magnet group produced two proof-of-principle configurations for the segmented configuration that made changes to the outer dimensions of the conductor (see figures 7 and 8 for field comparisons). The layout of the conductor was also changed, which perforce modifies the cross-section of the coil. In

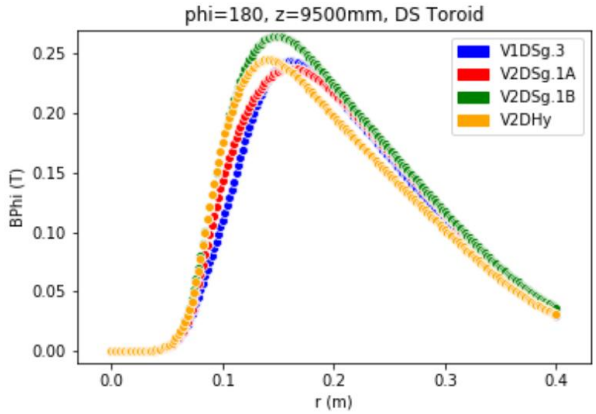

Figure 7 – *Total field vs. radius at the center of an open septant at z=9500mm for the different configurations. The radial distribution is slightly different in each case, but full simulations with modified detector tiles show that the optics is adequate in each case.*

addition, different sizes of water-cooling holes were considered. Thus there are 4 versions of the downstream torus that are compared in this document, all for 7-fold symmetric coils. All used the same version of the upstream torus (referred to in this document with the prefix V1U.2a – JLAB version 1.02A). Three of the configurations include segmented versions of the downstream torus, and one includes the JLAB version of the hybrid torus. The hybrid version has a suffix of V2DHy. The default segmented version is V1DSg3 (JLAB version 1.03) and the two new versions are V2DSg.1a and V2DSg.1b (JLAB versions have the same name).

The upstream magnet is matched to the Manitoba blocky model, but the the 125% current in the model itself (the BFIL factor of 1.25 in the simulation is not needed with this version). The default downstream magnet is the JLAB version of the segmented downstream magnet modified to match the inside surface of the initial Manitoba blocky model with the current density increased by ~15%. This coil was desgined to have double-pancakes for ease of winding the returns. The segmented subcoils 1, 2 and 3 have the same inner radii as the default but with a wider gap between pancakes (sub-millimeter) to account for 4% keystoning of conductor. The two versions have alternate subcoil 4 designs; V2DSg1.a is comprised of two 5 turn single pancake coils and V2DSg1.b has two 4 turn single pancake coils.

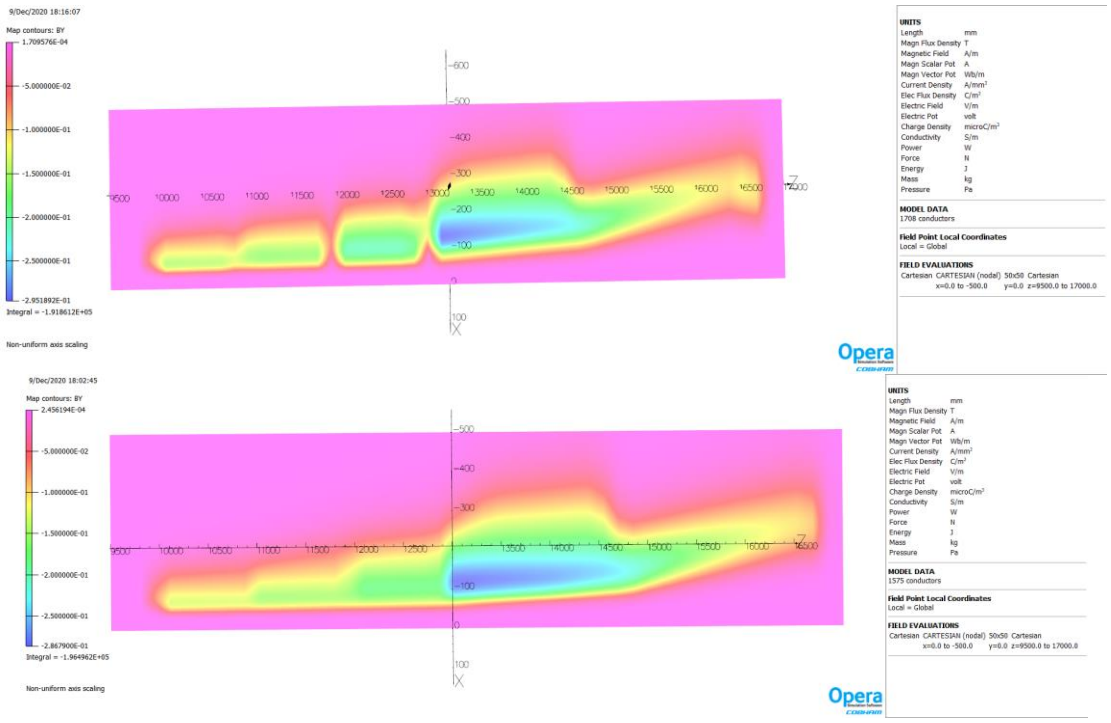

Figure 8 – *Total field for a plane at the center of an open septant for the segmented (top) and hybrid (bottom) downstream torus, produced in TOSCA. There are places along z where the total field drops to zero for the segmented torus due to the configuration having multiple separate coils. Note the color scale is slightly different for the two configurations.*

A more careful study of the impact of the small variations in the 3-D field map in the vicinity of the sub-coil boundaries will be carried out to carefully assess the differences between the hybrid and segmented conceptual designs. The goal would be to quantitatively understand the reasons for the relatively small differences in the deconvolution analyses given the fundamental difference of having one subcoil

winding at a subcoil boundary (hybrid case) as opposed to two windings with oppositely directed currents (segmented case). A finer spacing in the field map may be required to observe these differences. It should be noted that any effect would come from sub-dominant field components (the radial component of the field), that will act for a very short relative length of the magnet (<15%), and only act on components of the particle velocity that are not along z ($v_x, v_y \ll v_z$). Assuming there is an effect, it is expected that the hybrid would actually exhibit a larger difference from the maps we are currently using. The segmented has the kicks from opposite direction current returns one after the other while the hybrid has a much longer drift before the opposite kick happens. In consideration of this, the study is unlikely to cause a change in the conclusion that the segmented magnet is preferable to the hybrid.

2.3 Summary of the deconvolution studies

In order to determine the moller asymmetry, it will be necessary to measure dilutions as well as the asymmetries of the background processes. This is made possible due in part to the choice of detector tiling as shown in figure 1. In order to determine the moller asymmetry, it will be necessary to measure dilutions as well as the asymmetries of the background processes. This is made possible due in part to the choice of detector tiling as shown in figure 1.

Each detector tile will measure a total electron rate (and corresponding asymmetry) that is made up of different fractions corresponding to each physics process. We leverage both the radial and azimuthal dependence of each individual process to get maximal precision for the Møller asymmetry. The tiling has been selected such that we have a radial ring where the signal of interest dominates (ring 5) and others where the backgrounds dominate (for example ring 2 for the e-p Elastic process). The deconvolution is achieved through a simultaneous analysis of all tiles. Given the total rate and asymmetry in each tile and knowing the fraction of each individual process that contributes one can calculate the precision on each physics asymmetry. Due to the radial dependence of the e-p Inelastic asymmetry we have employed a scheme that separates this process into three distinct processes (W1, W2, W3) that each come with their own rate and asymmetry. The simulation allows us to quickly study additional backgrounds that can contribute to the rate, asymmetry, or both.

Table 1 – *Summary of the relative uncertainties in the asymmetries for each of the four models as determined in the de-convolution study.*

		Relative uncertainty			
	Process	V1U.2a_V1DSg3	V1U.2a_V2DHy	V1U.2a_V2DSg.1a	V1U.2a_V2DSg.1b
Primaries only	Møller	0.0211	0.0210	0.0212	0.0211
	e-p Elastic	0.0577	0.0560	0.0515	0.0614
	e-p Inelastic (W1)	0.1294	0.1529	0.1249	0.1370
	e-p Inelastic (W2)	0.0673	0.0681	0.0638	0.0709
	e-p Inelastic (W3)	0.1706	0.1658	0.1662	0.1742
Secondaries	Møller	0.0214	0.0214	0.0217	0.0215
	e-p Elastic	0.0631	0.0618	0.0560	0.0680
	e-p Inelastic (W1)	0.1495	0.1779	0.1413	0.1576
	e-p Inelastic (W2)	0.0804	0.0823	0.0752	0.0876
	e-p Inelastic (W3)	0.2309	0.2279	0.2313	0.2420

The results of the deconvolution studies confirm that we can achieve the same fractional uncertainty on the moller asymmetry regardless of the spectrometer configuration chosen, given that the detector tiling is adjusted to compensate for the slightly different features in the optics of each. The smaller variations in the background asymmetries are acceptable given the overall systematic error goals for the corrections. It is also highly likely that more detailed studies of tiling and all background contributions will further improve the performance once the final choice of final configuration has been made.

3. Engineering Criteria

3.1 Design Criteria

An extract from The Pugh matrix for the criteria that fall under design is shown in Table 2. It has been demonstrated via GEANT simulations that both the hybrid and segmented coil designs will satisfy the physics optics requirements. From an engineering perspective, both design approaches have matured sufficiently to confirm that all the engineering design goals – current density, temperature rise, water flow velocity and pressure drop can be met. Furthermore, we have also confirmed that by employing narrower conductors (i.e. rectangular instead of square and bent the hard way), we can still satisfy the engineering design goals while increasing clearances to the particle envelopes. In terms of the other criteria listed (e.g. power supply cost, number of joints, number of electrical solation breaks and so on), both designs are again very comparable.

Table 2 – *Design category of the Pugh matrix comparing the hybrid and segmented coil designs*

Criteria (Critical to Quality)	Criteria Rating or Weight (1 - 10)	HYBRID (BASELINE)	SEGMENTED	JUSTIFICATION FOR SCORE COMPARED TO BASELINE
DESIGN				
Satisfies all physics optics requirements	10	0	0	Confirmed by JM and KK that both designs satisfy physics requirements
Minimal local magnetic field 'anomalies' (e.g. near transitions and lead in/out)	6	0	0	Both coil designs are likely to have similar effects
Does not exceed temperature rise design target	6	0	0	Both coil designs satisfy design target
Does not exceed water flow velocity design target	1	0	0	Both coil designs satisfy design target
Does not exceed pressure drop design target	1	0	0	Both coil designs satisfy design target
Largest clearance between sub-coil bodies to particle envelopes	9	0	0	Latest clearance checks indicate both designs are very comparable
Largest clearance between sub-coil current leads and particle envelopes	9	0	0	Both coil designs are likely to be similar, as all leads exit from top of coils
Readily available conductor	4	0	0	Only off-the-shelf conductor (dies) have been selected for use
Lowest cost power supply	3	0	0	Both coil designs now have reduced kW requirements
Lowest number of brazed joints	3	0	0	Similar number for both designs
Lowest number of electrical isolation breaks	3	0	0	Similar number for both designs
Reduced technical complexity of coil design	7	0	1	Segmented: separate coils simplify the design
Least complicated coil support design	7	0	0	Support design for both coil designs are likely to have similar challenges
Lowest magntitude of dipole moment in bore for symmetric coil locations	10	0	0	No difference between hybrid and segmented as per JM
Least sensitivity of dipole magnitude in the bore for asymmetric coil locations	10	0	0	No difference between hybrid and segmented as per JM
Alignment fiducials located in optically accessible locations incorporated in design	7	0	0	Similar for both designs

3.2 Fabrication Criteria

The Pugh matrix for the operation and safety criteria is shown in Table 3. Primarily because of the use of separate coils for the segmented design, each coil will be easier to wind, apply ground wrap and pot. As the individual coils (the sub-coils) are relatively short compared to the sub-coils of the hybrid design, controlling coil fabricated dimensions should be easier requiring less complicated winding tooling, jigs and fixtures. Attaching water and electrical fittings should also be easier for the segmented design as will carrying out Quality Assurance and Quality Checks – e.g. hydraulic flow tests. In terms of production and delivery schedule, vendors have confirmed that both design types will have the same or very similar schedules. In terms of cost, the segmented design is approximately $47 K lower cost compared to the hybrid design. Refer to Section 4 for further details.

Table 3 – *Fabrication category of the Pugh matrix comparing the hybrid and segmented coil designs*

FABRICATION				
Ease of conductor cleaning prior to winding	1	0	0	Will be the same for individual conductors for both designs
Ease of insulating conductor immediately prior to winding	1	0	0	Will be the same for individual conductors for both designs
Ease of applying Ground wrap to conductor bundle (coil)	3	0	1	Segmented: More uniform coil cross-section along Z, separate coils
Ease of bending conductor during winding	3	0	1	Easier to control the wind of segmented (separate) coils
Minimal risk of damage to conductor inner channel during fabrication	7	0	1	Easier to control the wind of segmented (separate) coils
Ease of controlling coil dimensions during insulation and winding	7	0	1	Easier to control the wind of segmented (separate) coils
Reduced complexity of winding tooling, jigs and fixtures	6	0	1	Easier to control the wind of segmented (separate) coils
Ease of handling	5	0	1	Easier to handle small individual coils for segmented design
Reduced complexity of potting mold and any necessary fillers	5	0	1	Easier to control the potting of segmented (separate) coils
Coils are easier to pot (less tortuous resin flow paths)	5	0	1	Easier to control the potting of segmented (separate) coils
Reduced size of curing oven	3	0	1	One potential coil vendor does not have a large enough oven
Coils are easier to cure (reduced temperature gradient across cross-section)	5	0	1	Easier to control the potting of segmented (separate) coils
Ease of fitting water and electrical connections	5	0	0	Will be the same for individual conductors for both designs
Ease of joining power busbars to coils	5	0	0	Will be the same for individual conductors for both designs
Ease of fitting temperature sensors	5	0	0	Will be the same for both designs
Ease of carrying out dimensional checks with regards to tooling design	6	0	1	Easier to carry out for segmented (separate) coils
Ease of performing other QA/QC checks (flow, resistance, hipot) with regards to tooling design	5	0	0	Will be the same for both designs
Ease of transport from vendor to Jlab	3	0	1	Segmented: Shipping individual (shorter) coils is easier and less prone to transport damage
Lowest cost of coils (incl. shipping costs)	3	0	1	Based on budgetary estimates from vendors

3.3 Assembly Criteria

The Pugh matrix for the assembly criteria is shown in Table 4. Again, due to the separate coils for the segmented design, assembly should be easier, although final alignment may take a little more effort due to have to align more separate elements.

Table 4 – *Assembly category of the Pugh matrix comparing the hybrid and segmented coil designs*

ASSEMBLY				
Ease of handling	6	0	1	Segmented: Individual coils are easier to handle
Ease of aligning coils to strongback	7	0	0	Fewer coils for Hybrid, but smaller coils for Segmented so a wash
Ease of assembling coil+strongback assemblies into a complete magnet to meet alignment requirements	7	0	0	Smaller coils for Segmented will likely be flatter, Long Hybrid coil constrains Z alignment so again a wash
Ease of adjustment of coil to mitigate any fabrication out-of-tolerance	7	0	1	Segmented: easier to adjust individual coils
Number of independent alignments	5	0	-1	Segmented: More parts to align

3.4 Operation Criteria

The Pugh matrix for the operation and safety criteria is shown in Table 5. Both designs are very similar with regards to operation – i.e. forces, stresses and thermal growth are comparable. Although the segmented design may be prone to changes in alignment for the individual coils during operation, any misalignment can be assessed during the commissioning stage by energising the coils to full power in vacuum, waiting for thermal equilibrium and then de-energising, checking and re-aligning. The separate coils for the segmented design lend themselves relatively easily to individual alignment adjustment.

Table 5 – *Operation category of the Pugh matrix comparing the hybrid and segmented coil designs*.

OPERATION				
Minimal 'potato-chipping' due to temperature difference across coil	8	0	0	
Minimal sag due to gravity especially at coil ends	8	0	0	Similar for both designs
Minimal detrimental effects due to coil expansion due to temperature	8	0	0	
Lowest stresses from symmetrical arrangement of coils	7	0	0	Similar for both designs
Lowest stresses from asymmetrical arrangement of coils	7	0	0	Similar for both designs
Lowest stresses due to worst case fault scenario	7	0	0	Similar for both designs
Lowest induced voltages due to a sub-coil string failure	4	0	1	Hybrid: C1 develops 133 V, Segmented: Less than 1 V
Ease of coil replacement/swap out due to failure	6	0	1	Segmented: Easier to replace individual coils
Least likelihood that subcoil relative alignment changes during operation	9	0	-1	Segmented: Individual coils have a higher likelihood of moving
Ease of adjusting coils in the hall after low power beam run	7	0	1	Segmented: Individual coils and support system should provide more degrees of freedom for adjustment
Lowest life-cycle costs (includes costs to produce and operate)	5	0	0	Both coil designs now have reduced kW requirements
Ease of access to water/electrical fittings and instrumentation	6	0	0	Similar for both designs
Sufficient cooling power to handle coil heating due to beam, particles, radiation	6	0	0	Similar for both designs
Minimal complexity of protection system	7	0	0	Similar for both designs
Minimal technical complexity of control and instrumentation systems	7	0	0	Similar for both designs
Does not exceed design targets when operating at 10% higher than operating current	7	0	0	Similar for both designs

4. Schedule and Cost Impacts

Schedule impact

The one vendor who provided cost and schedule estimates for both designs confirmed that there would be no difference in schedule for coil delivery.

Table 6 – *Schedule for the delivery of each of the 7 coils, regardless of the configuration.*

DS Torus Production Coil #	Lead time ARO (weeks)
1	24
2	32
3	36
4	40
5	44
6	48
7	52

It is likely that additional time will be required for the segmented design as follows:

- Design: 3 weeks (coil strong backs, water-cooled leads and jumpers)
- Fabrication: 6 weeks (coil dies, water-cooled leads and jumpers, coil support and adjusters)
- Assembly: 2 weeks (alignment and survey of coils on strong back and frame)
- Installation: 1 week (alignment and survey)
- Testing and performance: 1 week (alignment and survey)

Cost Impact

Opting to use the segmented coil design impacts the cost as shown below primarily for the following reasons:

- Additional alignment time during assembly
- Additional alignment time during installation
- Additional alignment time during testing and performance

Table 7 – *Impact of utilizing the segmented configuration in $k or hours.*

Cost Category	$K or Hours
Materials	$52 K
Principal Engineer	100 hours
Senior Engineer	16 hours
Mechanical Engineer	90 hours
Mechanical Designer	100 hours
Technician	280 hours

5. Summary and Conclusion

The result of the Pugh matrix analysis is +84 in favor of the segmented option. Given that the weights can be somewhat subjective, the result was checked with equally weighted criteria, and the result is still in +17 favor of the segmented option. The results of implementing a finer field map to understand the relatively small differences between the hybrid and segmented are unlikely to change this decision. Therefore it is the recommendation of the Spectrometer Group that the MOLLER experiment move forward conditionally with a segmented configuration as the new baseline design for the spectrometer.

Appendix

A Pugh matrix is a simple tool for methodically making a choice from several alternatives. "Pugh" comes from its originator, Stuart Pugh. It is most useful when there are two viable choices and there is poor buy-in from different members of a team, or if there is a design decision or policy that keeps being attacked or reconsidered. A set of criteria relevant to the choice of alternatives are listed. Each criterion receives a weight factor (1-10) denoting its relative importance compared to the other criteria, and then the alternatives are scored (-1, worse or +1 better) relative to the baseline (scored as 0). The team members then attempt to agree on the relative weights and the scores. Although the weighting may still be somewhat subjective, the scoring is less so. If the total for an alternative is negative, that means it is worse than the baseline.

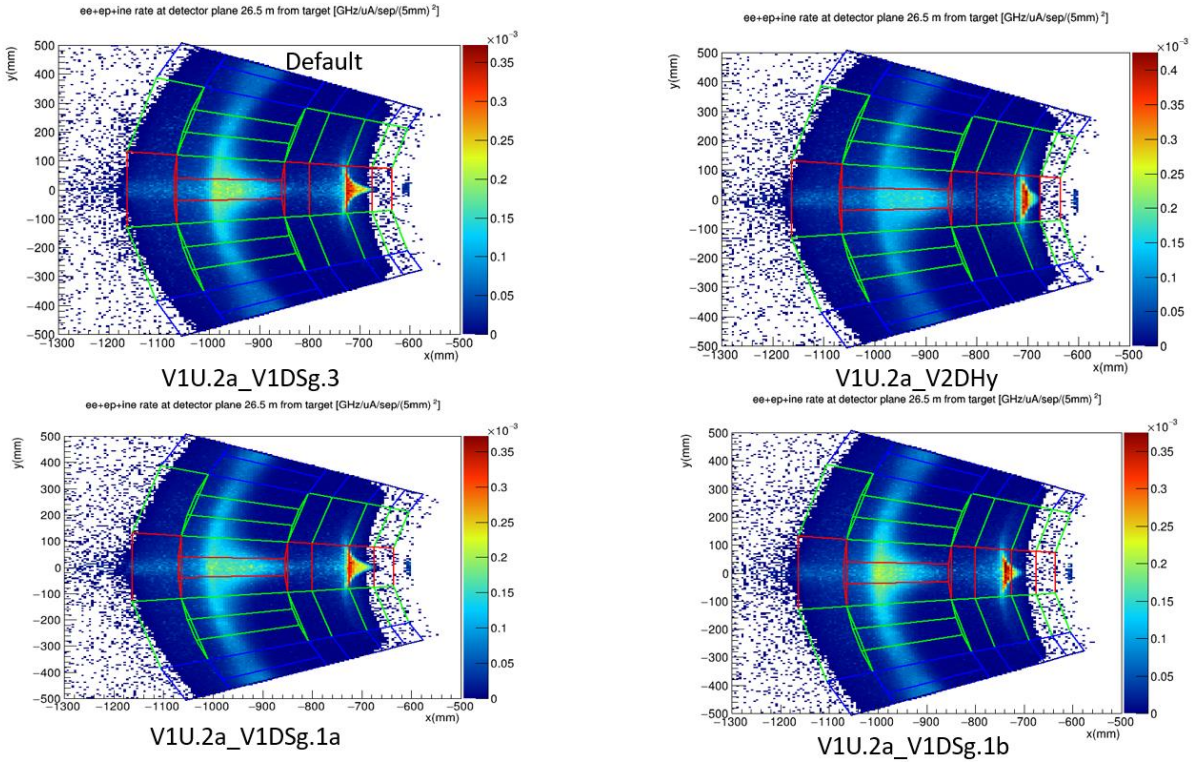

Figure A.1 – *Comparison of the 2D rate weighted distributions for two segmented magnets (bottom plots) and an alternative hybrid magnet (top right). The default from figure 1 is reproduced in the upper left.*

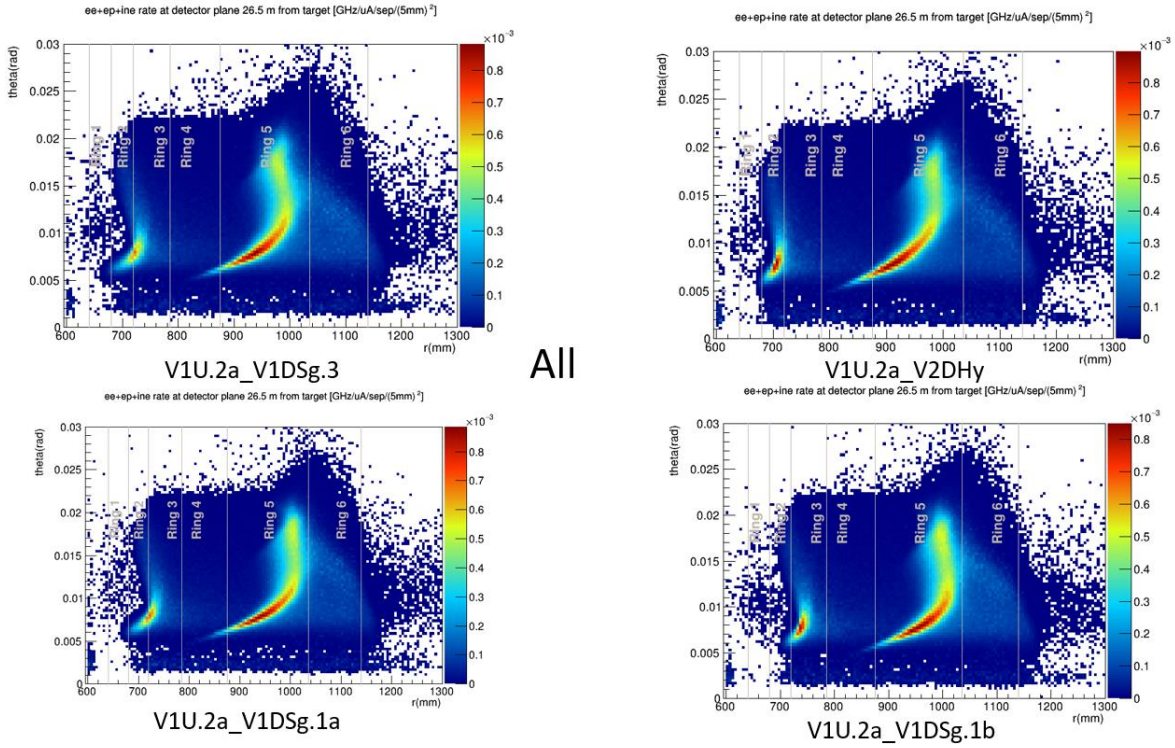

Figure A.2 – *Comparison of the rate weighted theta-r distributions for two segmented magnets (bottom plots) and an alternative hybrid magnet (top right). The default from figure 2 is reproduced in the upper left.*

Name	Asymmetry	uncert[ppb]	relative uncer[ppb]
moller	-34.2891	0.7226	-0.0211
epElastic	-21.7975	1.2567	-0.0577
epInelasticW1	-537.7265	69.5601	-0.1294
epInelasticW2	-537.9042	36.2037	-0.0673
epInelasticW3	-447.5959	76.3651	-0.1706

V1U.2a_V1DSg.3

Name	Asymmetry	uncert[ppb]	relative uncer[ppb]
moller	-34.6893	0.7291	-0.0210
epElastic	-23.8224	1.3331	-0.0560
epInelasticW1	-565.0421	86.4192	-0.1529
epInelasticW2	-541.4439	36.8601	-0.0681
epInelasticW3	-469.0352	77.7575	-0.1658

V1U.2a_V2DHy

Name	Asymmetry	uncert[ppb]	relative uncer[ppb]
moller	-34.6953	0.7339	-0.0212
epElastic	-24.0622	1.2393	-0.0515
epInelasticW1	-581.0825	72.5628	-0.1249
epInelasticW2	-556.3365	35.4930	-0.0638
epInelasticW3	-477.5756	79.3916	-0.1662

V1U.2a_V2DSg.1a

Name	Asymmetry	uncert[ppb]	relative uncer[ppb]
moller	-34.2668	0.7220	-0.0211
epElastic	-22.8270	1.4016	-0.0614
epInelasticW1	-542.3427	74.3137	-0.1370
epInelasticW2	-536.8306	38.0518	-0.0709
epInelasticW3	-450.8812	78.5307	-0.1742

V1U.2a_V2DSg.1b

Figure A.3 – *Deconvolution results for five processes for each of the 4 downstream torus conductor configurations. These results are for simulations which do not include secondary particle production.*

Name	Asymmetry	uncert[ppb]	relative uncer[ppb]
moller	-34.1199	0.7314	-0.0214
epElastic	-22.1256	1.3971	-0.0631
epInelasticW1	-623.6047	93.2303	-0.1495
epInelasticW2	-607.8443	48.8750	-0.0804
epInelasticW3	-452.7696	104.5314	-0.2309

V1U.2a_V1DSg.3

Name	Asymmetry	uncert[ppb]	relative uncer[ppb]
moller	-34.5202	0.7396	-0.0214
epElastic	-23.5685	1.4564	-0.0618
epInelasticW1	-628.5779	111.8160	-0.1779
epInelasticW2	-602.9652	49.6308	-0.0823
epInelasticW3	-472.8495	107.7454	-0.2279

V1U.2a_V2DHy

Name	Asymmetry	uncert[ppb]	relative uncer[ppb]
moller	-34.5291	0.7489	-0.0217
epElastic	-23.9641	1.3417	-0.0560
epInelasticW1	-651.7935	92.1016	-0.1413
epInelasticW2	-615.7681	46.3195	-0.0752
epInelasticW3	-481.1127	111.2654	-0.2313

V1U.2a_V2DSg.1a

Name	Asymmetry	uncert[ppb]	relative uncer[ppb]
moller	-34.0727	0.7326	-0.0215
epElastic	-23.0626	1.5689	-0.0680
epInelasticW1	-615.1191	96.9158	-0.1576
epInelasticW2	-611.7688	53.6000	-0.0876
epInelasticW3	-455.2799	110.1924	-0.2420

V1U.2a_V2DSg.1b

Figure A.4 – *Deconvolution results for five processes for each of the 4 downstream torus conductor configurations. These results are for simulations which include secondary particle production.*